

**RADIATION ENVIRONMENT
AT THE LHCb VERTEX DETECTOR AREA**

V. Talanov
Institute for High Energy Physics, Protvino, Russia

LHCb collaboration

Abstract

Particle fluxes and absorbed dose levels in the LHCb Vertex Detector are presented. The simulation is performed with the IHEP MARS program and includes all the material of the Vertex Detector together with supporting structures as well as the surrounding LHC and LHCb elements. The particle spectra are presented as a function of radius and momentum, and have been converted to a 1 MeV equivalent neutron flux by folding them with the induced displacement damage constant tables.

*) E-mail: talanov@mx.ihp.su

1 Introduction

The LHCb Vertex Detector [1] consists of 17 stations, each station being composed of two $150\text{ }\mu\text{m}$ thick silicon discs, and will be installed inside a vacuum tank around the interaction region of IP8. The detectors are placed perpendicular to the beam axis, and the radial coverage of the sensitive area of the silicon will be from 1 to 6 cm. Although LHCb will operate at a moderate luminosity of $2 \times 10^{32}\text{ cm}^{-2}\text{ s}^{-1}$ the position of the stations extremely close to the beam line will result in significantly high charged particles fluxes and hence absorbed dose levels in the material of the detector. The position of the interaction point of LHCb is inside the LHC tunnel, leading to a radiation environment different from the one in vertex detectors of other LHC experiments.

This note is organised as follows. The next section will describe the material included in the simulation. Sections 3 deals with the simulation program and the event generators. Section 4 shows the main particle spectra. In section 5 the convolutions of the induced damage constant tables is presented, leading to the 1 MeV equivalent neutron fluxes in the complete geometry of vertex detector.

2 Vertex Detector Geometry

The description of the Vertex Detector geometry is as close as possible to the SICB geometry description [6] of version 1.11 taking into account the different approaches to the geometry description used in MARS and SICB.

The material of the 17 stations of Vertex Detector was divided radially into three parts. From 1 cm to 6 cm along the radius (distance from beam line) each station has $300\text{ }\mu\text{m}$ of silicon, followed by $900\text{ }\mu\text{m}$ of Be up to 12 cm, and then Cu/C (50%/50%) mixture to the 17.4 cm, which is the inner radius of the first vertex tank. In addition each station from both sides was covered by an Al-foil of $100\text{ }\mu\text{m}$ thick. All material which is thought to contribute significantly to the total particle flux has been included in the model according to the engineering drawing as shown in Fig. 1. The stations are placed in a stainless steel tank connected by six plates to a second outer tank of 45 cm radius. The top of the outer tank consists of a 9.5 cm thick aluminium plate, and includes a model of the two motors and support details.

The area upstream of the Vertex Detector includes a 3.34 m long LHC beam pipe (5 cm radius and 1 mm thick stainless steel) connected to the compensation dipole which in a crude approximation was simulated as a 1×0.77 m block of iron with an inner hole of 0.6×0.05 m positioned at 3.33 m from IP8 ¹⁾. Downstream a description of the LHCb elements is included like the iron shielding plate of the LHCb magnet. The area was surrounded by the LHC tunnel made of heavy concrete ($\rho = 3.64\text{ g/cm}^3$) positioned according to the experimental area design drawings ²⁾.

3 Event Generators and Simulation

The results of the particle flux, spectrum, and absorbed dose levels have been obtained with the IHEP MARS [2] program. Most of the Monte-Carlo simulations were done using 10 MeV energy threshold for all hadrons except neutrons and 100 keV for electrons and photons. A small test run was made with the hadron energy threshold reduced to 1 MeV, this does not lead to a significant difference in the results. Neutrons were

¹⁾ The precise position and type of this dipole has not been fixed yet, but an educated guess has been made by Georg von Holtey

²⁾ Engineering drawings of LHCb experimental area and interface to the LHC were kindly provided by D. Lacarrère

transported down to the thermal energy (10^{-5} eV) to include possible contribution to the charged particles flux from the electrons due to the 'n- γ capture' channel.

The Monte-Carlo simulations are based on a pre-recorded set of minimum bias events obtained from the DPMJET-II event generator [3]. DPMJET-II is known to be the most recent dual parton model generator and is an update to the older DTUJET93 program [4], and is specially suited for simulation of minimum bias hadronic collisions.

For physics analysis studies the LHCb simulation program (SICB) uses another event generator, PYTHIA 5.7 [5]. A comparison between generators can be found in ref. [7]. It shows that DTUJET and PYTHIA produce events with quite different characteristics. In particular PYTHIA with standard setting produces up to 50% more primary particles compared to DTUJET93.

Although this work is not aimed to the discussion of the primary particles event generator choice for the background studies the difference mentioned above implies an uncertainty of at least 50% to the results presented below, besides the statistical error that comes from Monte-Carlo simulations and which is in the order of 30%.

4 Overview of the results

The fluxes of charged hadrons, neutrons and photons as a function of the distance from the beam axis and vertex station number are presented in Fig.2–4. The data presented on these figures are normalised per 1 interaction in the IP8.

Fig.5 gives the absorbed dose level for a luminosity of $5 \times 10^{32} \text{ cm}^{-2} \text{ s}^{-1}$.

The flux seems to be independent from the position of the stations along the beam line. Fig. 6 shows the particle flux for a station close to the mean position of the interaction point (station 6). The figure also shows a comparison of primary and total particles flux. At small radii the flux is dominated by particles originating in the primary interaction, while at a radius of 6 cm roughly 30% of the flux is due to neutrons.

Figures 7 and 8 give particle spectra at stations 6 and 17 respectively, at a radius of 1 cm from the beam line. Station 17 is located 78 cm downstream from the IP. These figures show the variation of the particles momentum distribution along the Z axis.

Fig.9 gives the comparison of the results expressed in 1 MeV equivalent neutron flux, obtained after folding the spectra with particle induced displacement damage constants.

4.1 Charged Particle flux

The charged hadron flux is given in Fig.2. There is little difference in the total charged hadron flux between the stations. The mean value of the flux is about 0.8 charged hadrons/cm² per one p-p interaction in the IP. The radial dependence of the charged hadron flux follows the $a(z)/r^2$ rule with the factor $a(z)$ almost constant along Z axis.

The difference between the flux of the primary charged hadrons (i.e. originating in the p-p interaction in the IP) and total charged hadron flux that includes all the secondaries is small. This is because the amount of material placed close to the beam line ($\approx 0.6\%$ of radiation length per vertex station) is insufficient for the primaries to start multiple hadron cascades, and hence the flux of the secondary hadrons is a small fraction of the primary flux. Care has been taken in the design to place all heavy support structures at larger radii, i.e. at the low particle flux environment. This is valid only for the charged particles. The situation for the neutrons is quite different and is discussed in the next section.

From the particle spectra presented on Fig.7 and 8 one can see that the charged hadron flux is dominated by pions. Pions constitute about 90% of the total charged hadron

flux and thus are mainly responsible for the radiation damage, discussed in section 5. The flux of all the rest hadrons is in fact only a small addition to the pion flux.

Absorbed dose levels, given in Fig.5, are normalised to a interaction rate of 4×10^7 events/s, which corresponds to luminosity of $5 \times 10^{32} \text{ cm}^{-2} \text{ s}^{-1}$ for one operational year of 10^7 s. Under these conditions the maximal value of absorbed dose in the silicon of vertex stations appeared to be about 10⁷ Rad/year at 1 cm radius, and 200 krad/year at the location of the front-end electronics.

It should be noted that the contribution of the electrons to the flux of charged particles in the vertex detector area appeared to be negligible. This is caused first by the absence of primary electrons originating directly in the p-p interaction. In addition the amount of material in the Vertex Detector area is too small to enable the production of electron-photon showers by the primary particles or the thermal neutrons — from the 'n- γ capture' channel. Nevertheless the contribution of secondary electrons to the radiation dose was taken into account.

4.2 Neutron flux

The neutron flux is partly due to the specific position of the Vertex Detector. Since the LHCb collision point is positioned inside the LHC tunnel the vertex detector is surrounded by the concrete walls of the tunnel which are a source of secondary neutrons, hence not profiting from the open geometry like the downstream part of the spectrometer. At the silicon detectors the dominant flux is still due to primary particles, however at the position of the front-end electronics (at a radius of 7 cm) the neutron flux contributes about half of the total flux.

Fig.6 shows that while the charged hadron flux rapidly decreases with the increase of the radius, the secondary neutron flux remains almost constant. This is due to the LHC tunnel that serves as a waveguide for the neutrons produced in the hadronic interactions in the LHC beam pipe and compensation dipole front surface. Spreading inside the tunnel these neutrons dominate the total particle flux at higher radii and determine the radiation environment in these regions.

Hence all elements placed inside the tunnel like the first two tracking stations and RICH1 will have the same neutron flux of about 0.01 neutrons/cm⁻² per interaction, almost independent of radius and position along the beam-line. This flux could be reduced by coating the LHC tunnel walls by a material able to stop neutrons.

5 Particles Induced Displacement Damage

The expected damage in the silicon detectors due to a mixture of different particle types with different momenta can be estimated by folding the spectra with their induced displacement damage constants ³⁾.

Particles spectra from Fig.7 and 8 served as an input for the folding with the constants. As it was shown in section 4 the flux in the silicon of the stations is dominated by pions. Muons from pion and kaon decays are not included, but they make a negligible contribution to the displacement damage, as well as electrons.

The 1 MeV equivalent neutron flux/cm² for stations 6 and 17 is given in Fig.9. The difference in the particles spectra for these stations determines the difference in the induced displacement damage. While the absolute values of total hadron flux for these two stations are quite equal the spectra of all particles types for station 17 are much harder.

³⁾ The numerical data was kindly supplied by G. Lindstroem as compiled by ROSE collaboration

As known from [8] the most damaging pion energy is between 10 and 100 MeV while for protons the induced displacement damage increases with decreasing energy [9]. Hence the 1 MeV equivalent neutron flux is about 25% larger in station 6 compared to station 17.

The value of 1 MeV equivalent neutron flux is close to 0.5 neutrons/cm² per one interaction at a radius of 1 cm, or $\approx 10^{14}$ neutrons/cm²/year at the nominal LHCb luminosity 2×10^{32} cm⁻² s⁻¹ with an inelastic non-diffractive cross section of 80 mb. The PYTHIA generator with standard settings would give a value which is about 50% larger since the total flux is dominated by primary particles.

Acknowledgements

V. Talanov would like to express his gratitude to H. J. Hilke, T. Nakada and G. von Holtey for the support of this work, H. Dijkstra and the whole LHCb vertex community for the support and co-operation, and to D. Lacarrère for the significant help with the LHCb experimental area engineering drawings.

References

- [1] LHC-B Letter of Intent, CERN/LHCC 95-5, August 1995.
- [2] I. Azhgirey, I. Kurochkin and V. Talanov, “Development of MARS Code Package for Radiation Problems Solution of Electro–Nuclear Installations Design”, in: Proc. of XV Conference on Charged Particles Accelerators, Protvino, October 22-24 (1996); also MARS program WWW page at <http://wwwinfo.cern.ch/~talanov>.
- [3] J. Ranft, “DPMJET-II, a Dual Parton Model event generator for hadron–hadron, hadron–nucleus and nucleus–nucleus collisions”, in: Proc. of SARE2 Workshop, CERN, October 9–11, 1995; CERN/TIS-RP/97-05.
- [4] P. Aurenche *et al.*, Computer Physics Commun. **83** (1994) 3236.
- [5] H.U. Bengtsson and T. Sjöstrand, Computer Physics Commun. **46** (1986) 43; T. Sjöstrand, CERN-TH.7112/93.
- [6] D. Steele, “The R– ϕ Silicon Vertex Detector Simulation as Implemented in SICB”, LHCb 98-004, TRAC.
- [7] M. Huhtinen and C. Seez, CERN CMS/TN 95-133, September 27, 1995.
- [8] M. Huhtinen and P.A. Aarnio, NIM A **335** (1993) 580.
- [9] G.P. Summers *et al*, IEEE NS **40** (1993) 1372.

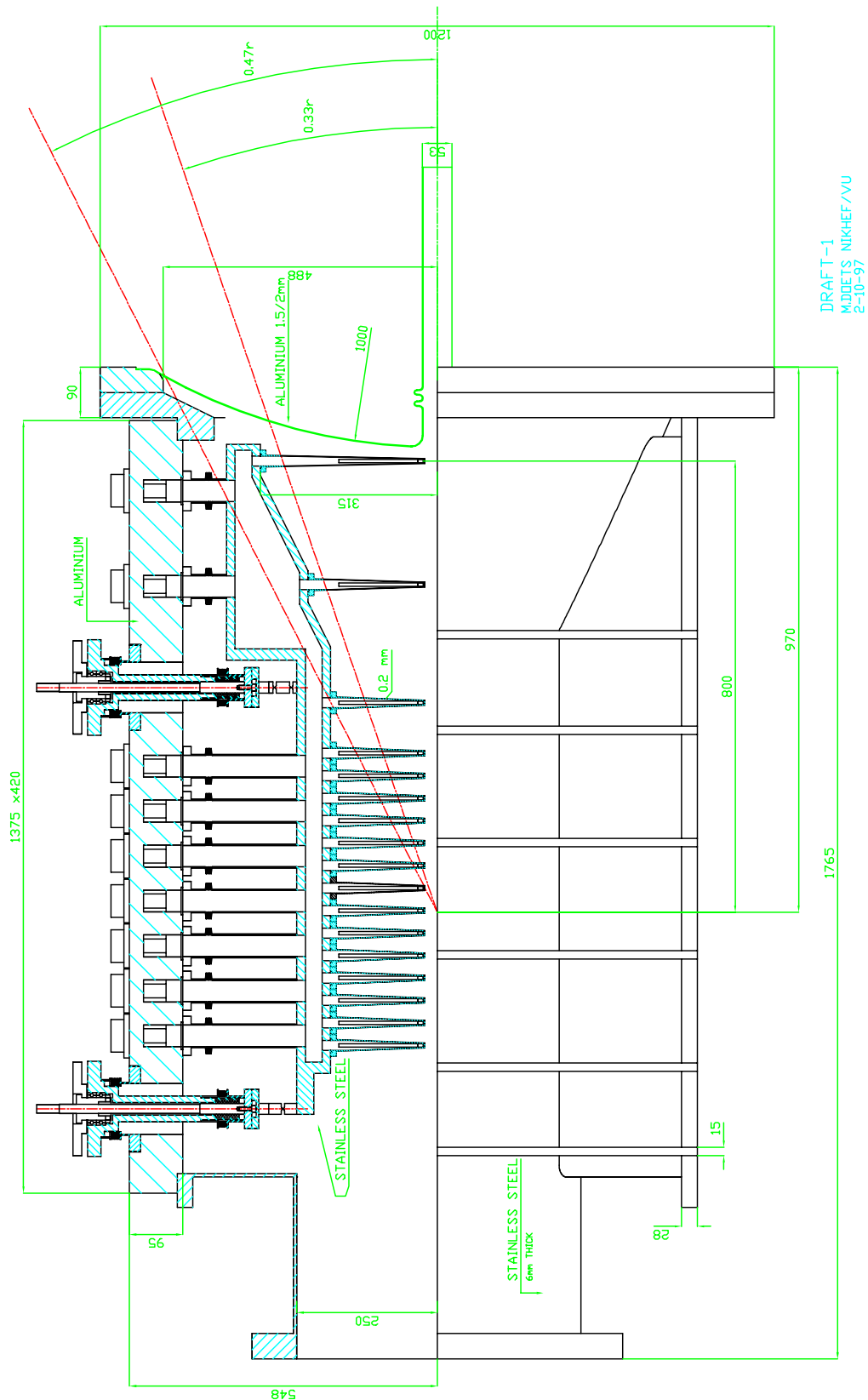


Figure 1: An overview of the vertex detector design.

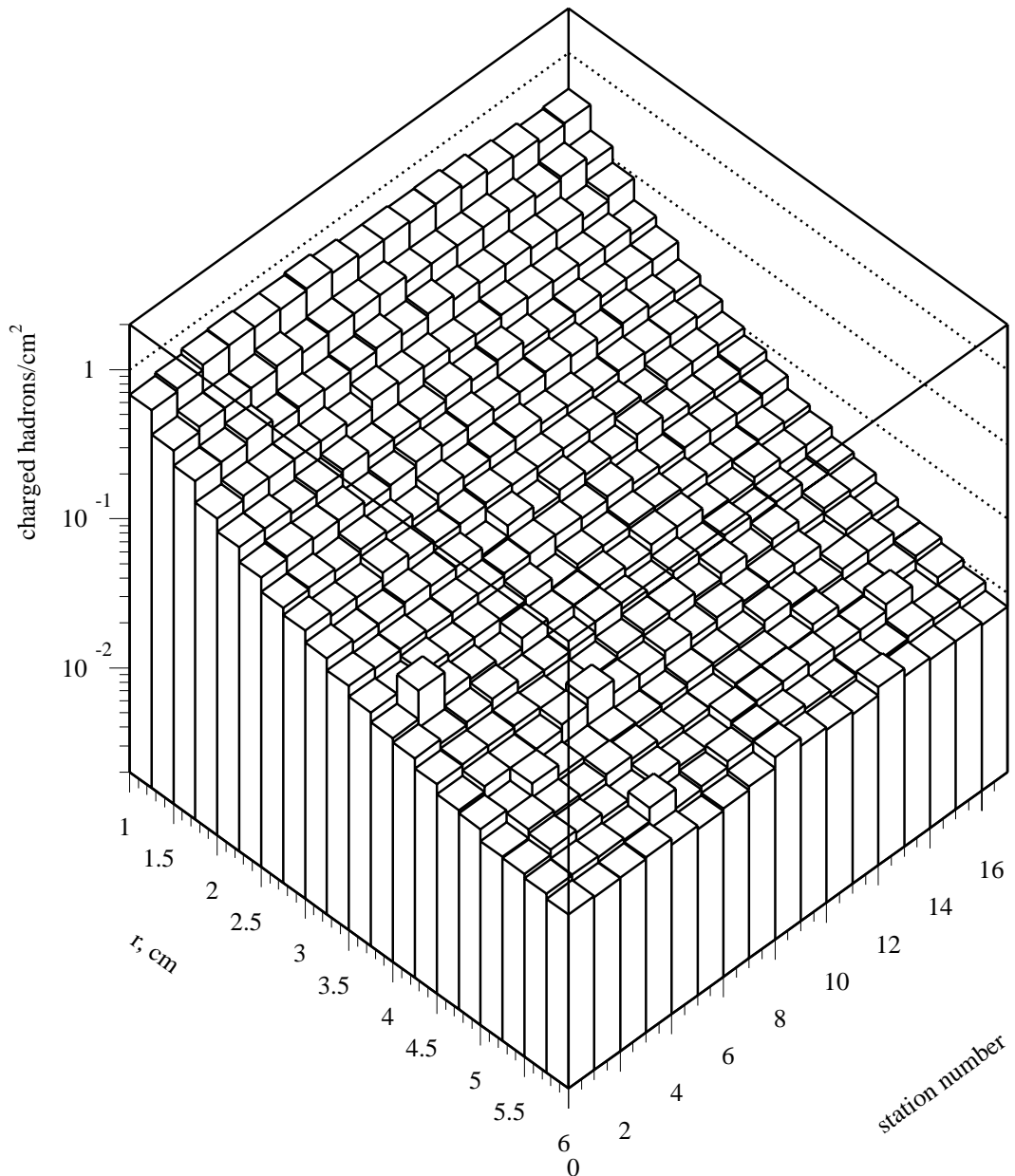


Figure 2: Vertex detector charged hadron flux map, particles/cm², as a function of distance from beam axis (*r*, left axis) and vertex station number (right axis).

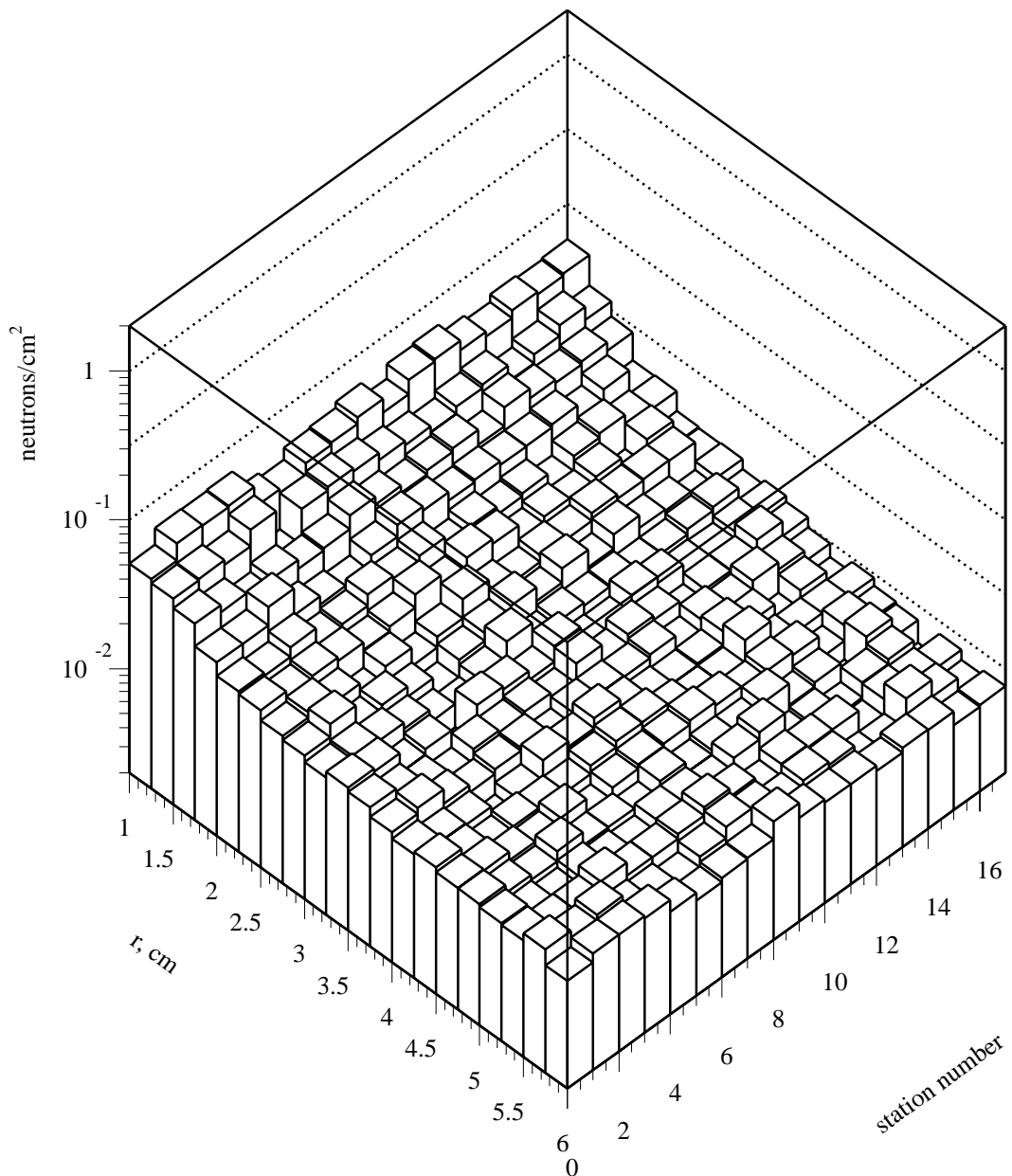


Figure 3: Vertex detector neutron flux map, particles/cm², as a function of distance from beam axis (r , left axis) and vertex station number (right axis).

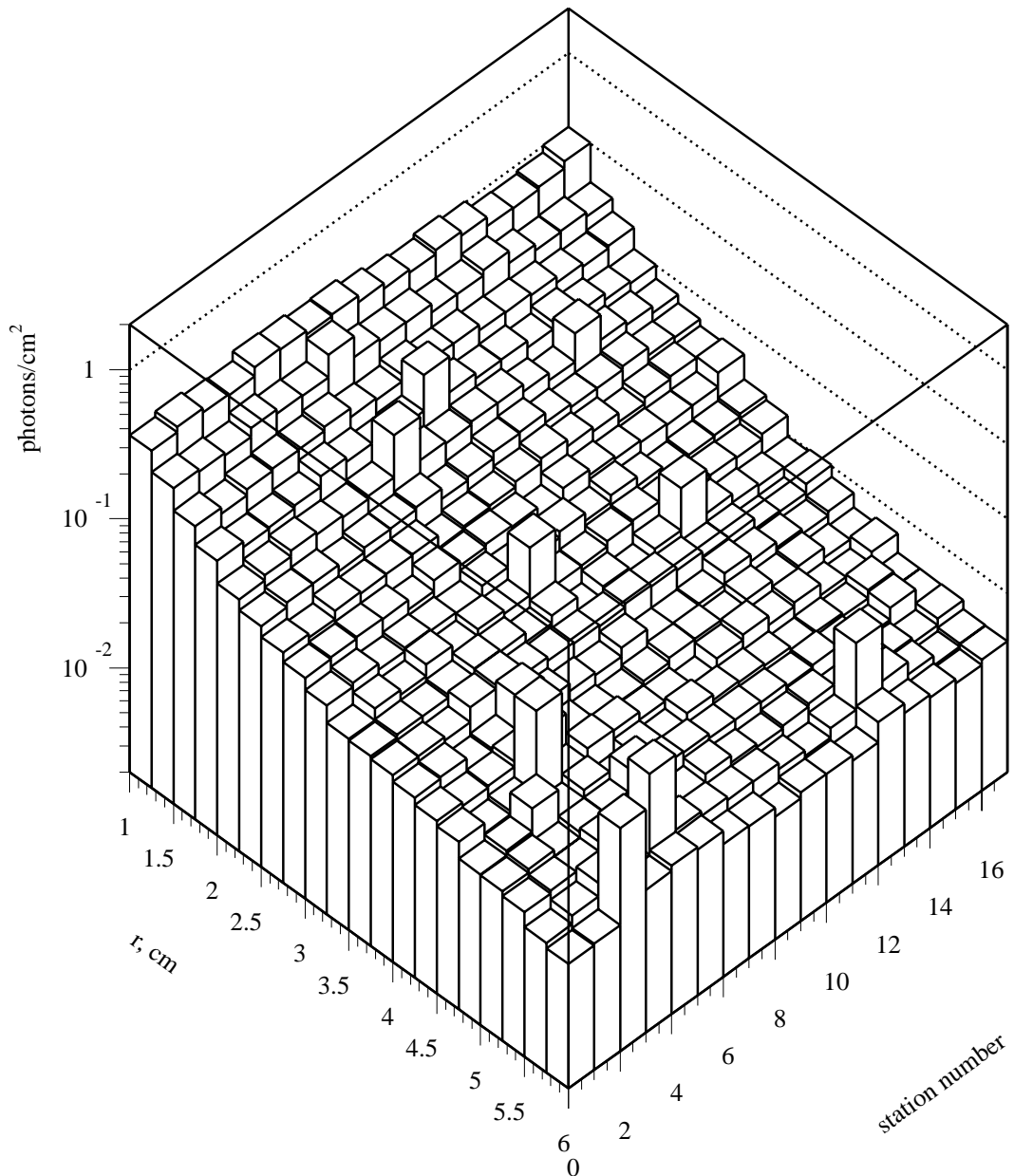


Figure 4: Vertex detector photons flux map, particles/cm², as a function of distance from beam axis (r , left axis) and vertex station number (right axis).

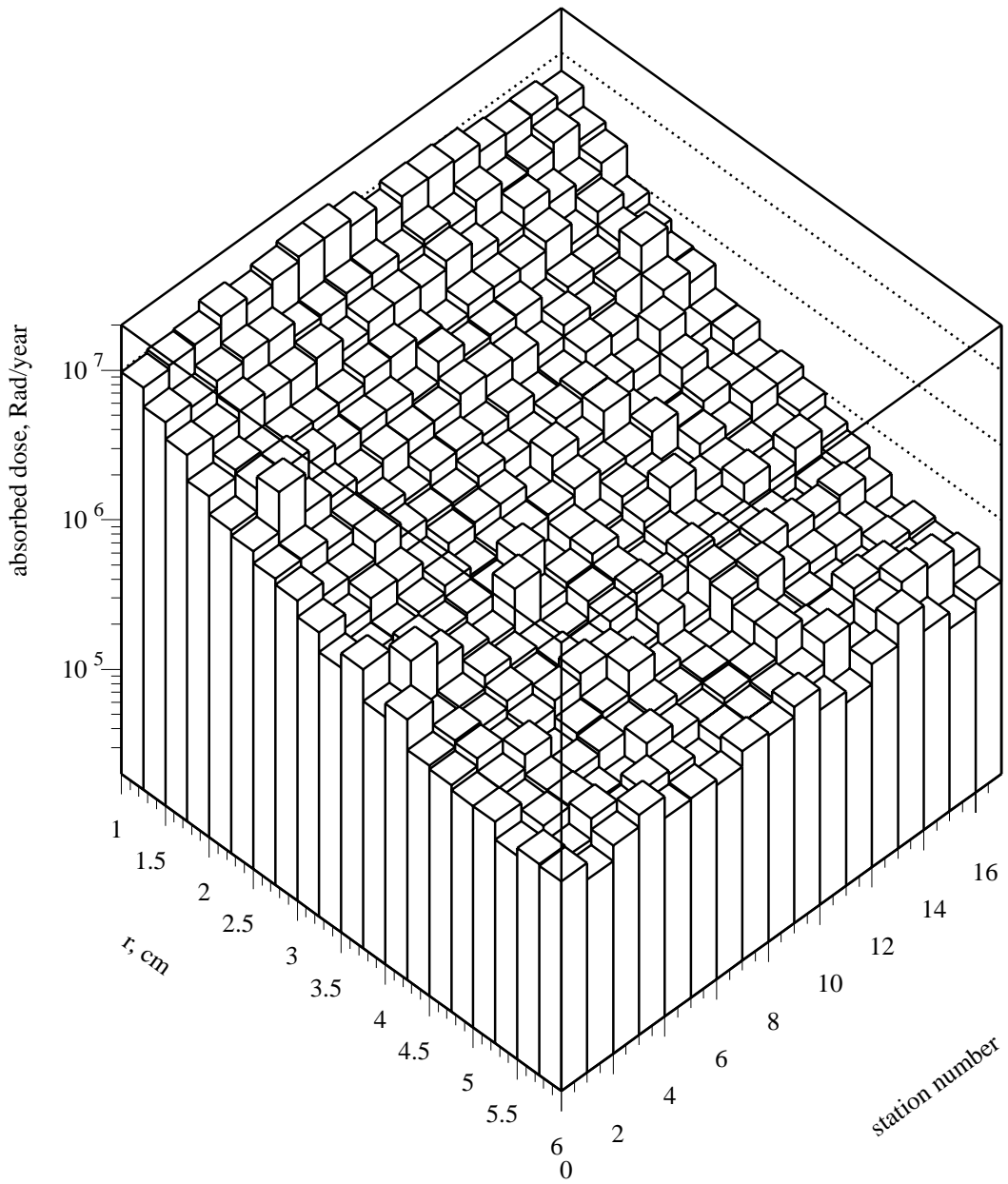


Figure 5: Vertex detector absorbed dose levels map, Rad/year, for the IP8 interaction rate of 4×10^7 events/s (that corresponds to luminosity of $5 \times 10^{32} \text{ cm}^{-2} \text{ s}^{-1}$) and a detector operational year of 10^7 s, as a function of distance from beam axis (*r*, left axis) and vertex station number (right axis).

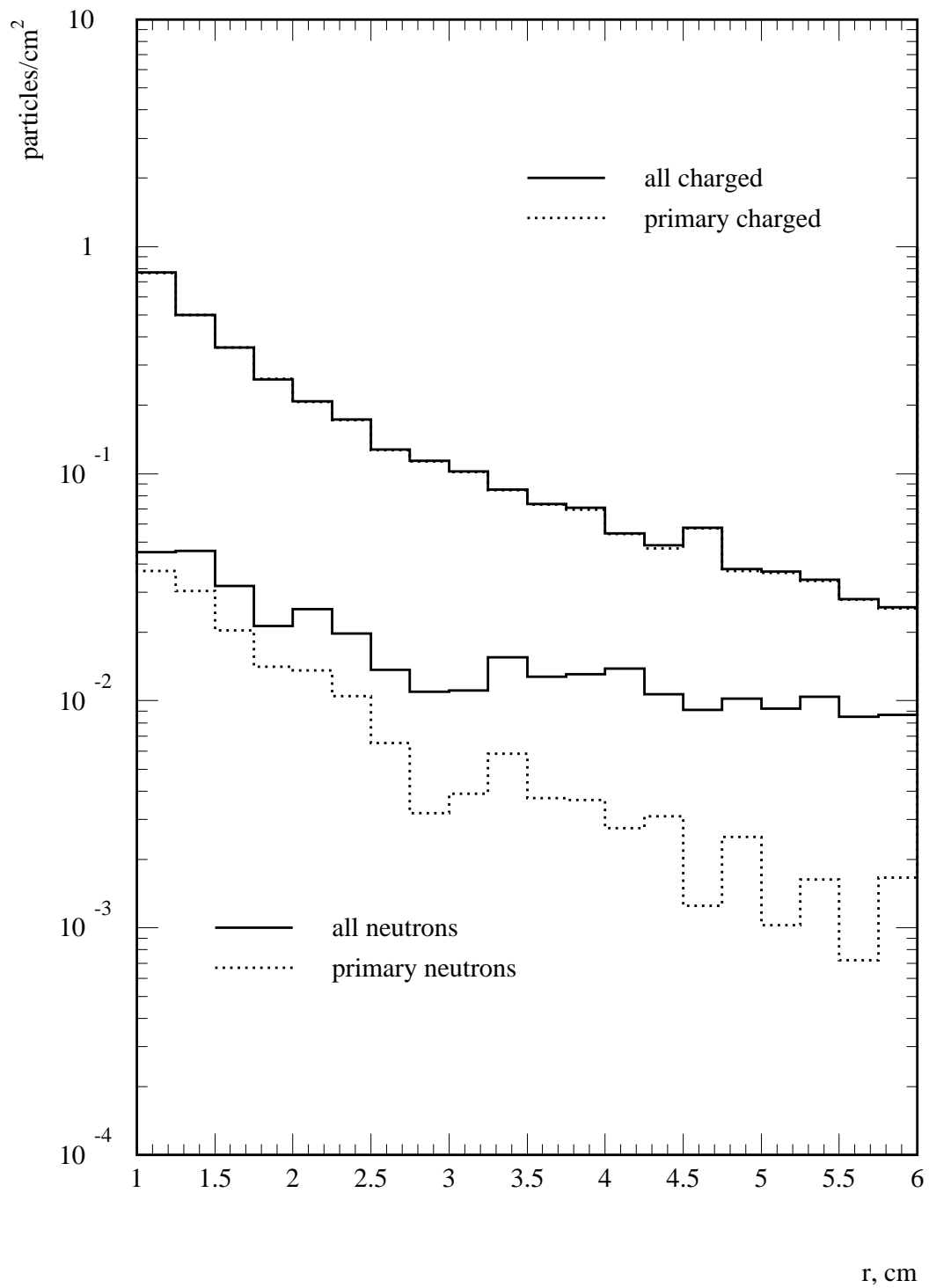


Figure 6: Total charged hadron and neutron flux (solid lines) and primary (coming from the p-p interaction in the IP8) charged hadron and neutron flux (dotted) at vertex station 6 normalized per 1 interaction in the IP.

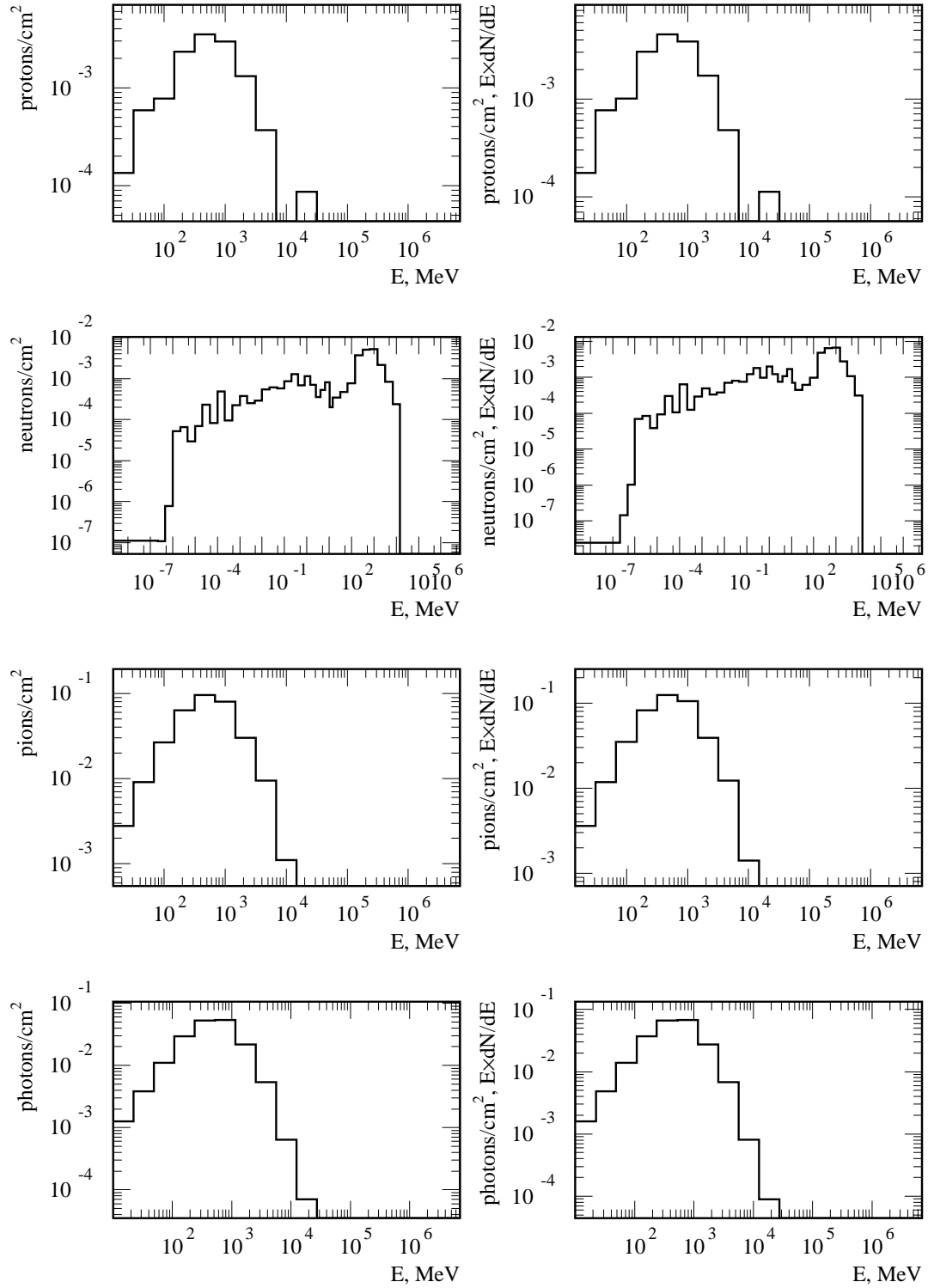


Figure 7: Proton, neutron, pion and photon spectra at vertex station 6 at a radius of 1 cm from the beam line normalised per 1 interaction in the IP.

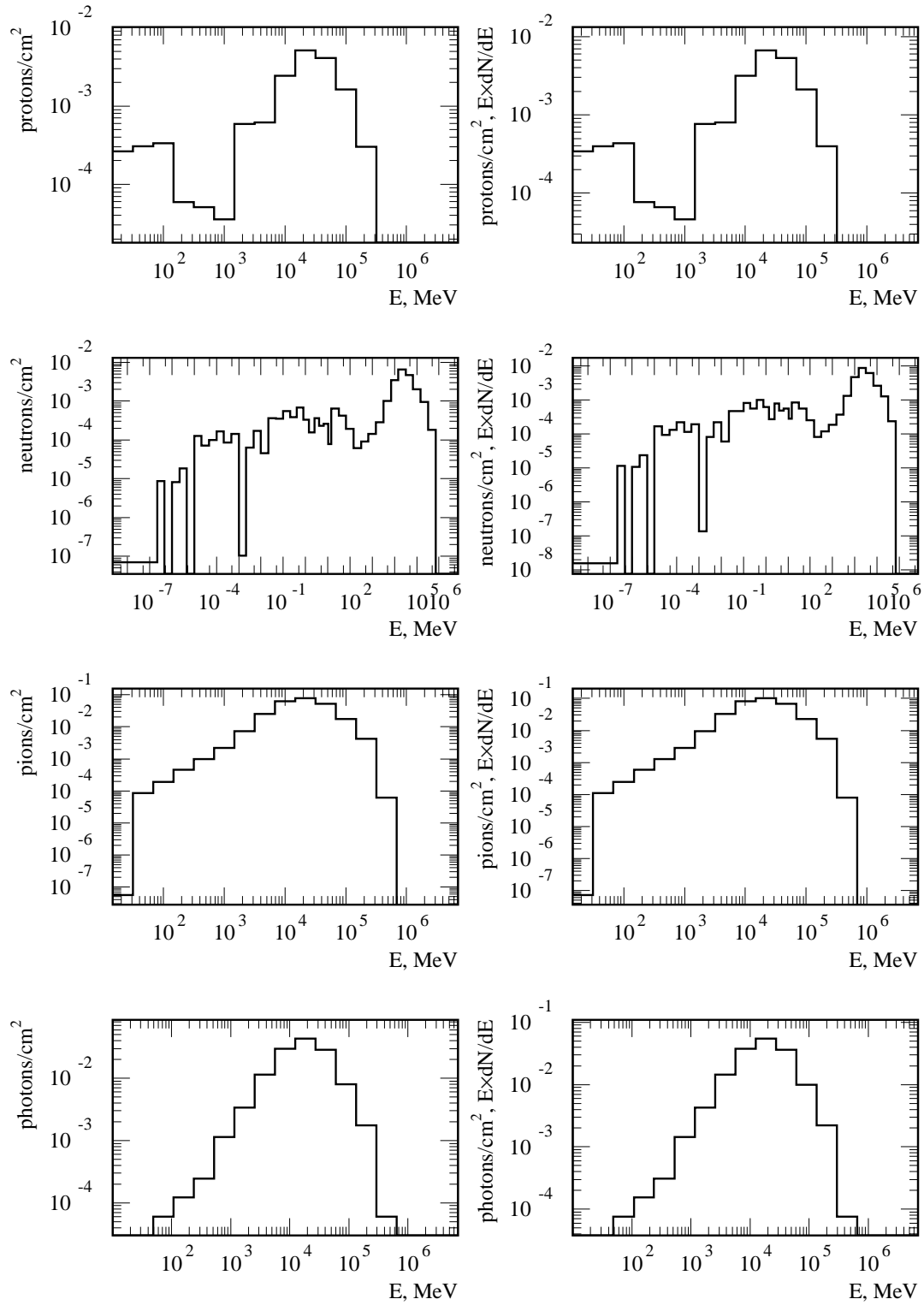


Figure 8: Proton, neutron, pion and photon spectra at vertex station 17 at a radius of 1 cm from the beam line normalised per 1 interaction in the IP.

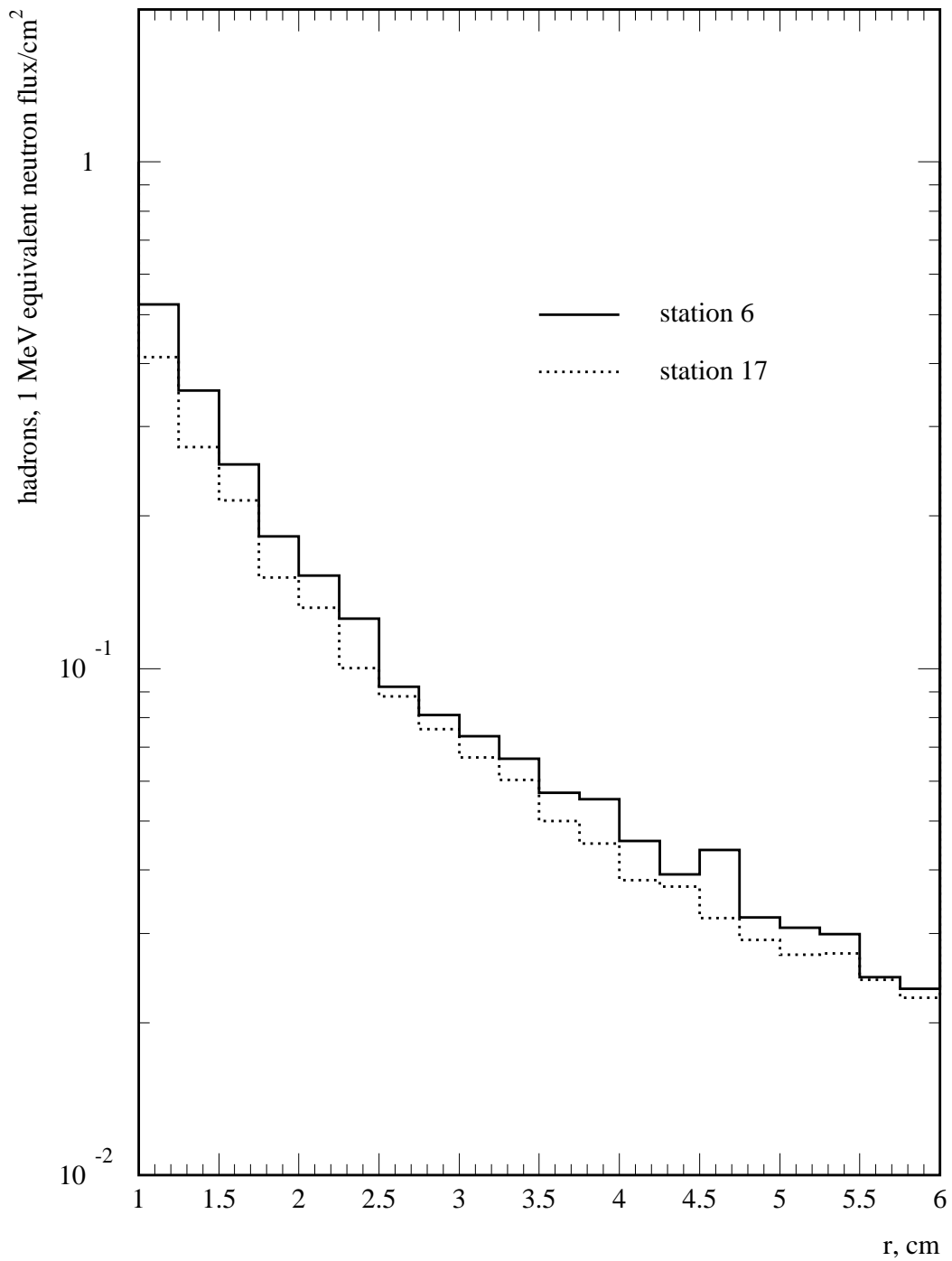


Figure 9: Total hadrons 1 MeV equivalent neutron flux, particles/cm², at vertex stations 6 (solid) and 17 (dotted) normalized per 1 interaction in the IP.